Author(s): Owen, Patrick J.; Hart, Nicolas H.; Latella, Christopher; Hendy, Ashlee M.; Lamon, Séverine; Rantalainen, Timo

Title: Identifying and Assessing Inter-Muscular Fat at the Distal Diaphyseal Femur Measured by Peripheral Quantitative Computed Tomography (pQCT)

Year: 2021

Version: Accepted version (Final draft)

Please cite the original version:

Owen, P. J., Hart, N. H., Latella, C., Hendy, A. M., Lamon, S., & Rantalainen, T. (2021). Identifying and Assessing Inter-Muscular Fat at the Distal Diaphyseal Femur Measured by Peripheral Quantitative Computed Tomography (pQCT). Journal of Clinical Densitometry, 24(1), 106-111. https://doi.org/10.1016/j.jocd.2019.11.001

Identifying and assessing inter-muscular fat at the distal diaphyseal femur measured by peripheral Quantitative Computed Tomography (pQCT).

Patrick J. Owen, PhD[1]; Nicolas H. Hart, PhD[2,3,4]; Christopher Latella, PhD[5]; Ashlee M. Hendy, PhD[1]; Séverine Lamon, PhD[1]; Timo Rantalainen, PhD[1,2,3,4,6]

[1] Deakin University, Institute for Physical Activity and Nutrition (IPAN), School of Exercise and Nutrition Sciences, Geelong, Victoria, Australia.

[2] Exercise Medicine Research Institute, Edith Cowan University, Perth, W.A., Australia.

[3] Institute for Health Research, University of Notre Dame Australia, Perth, W.A., Australia.

[4] Western Australian Bone Research Collaboration, Perth, W.A., Australia.

[5] Neurophysiology Research Laboratory, School of Medical and Health Sciences, Edith Cowan University, Perth, W.A., Australia.

[6] Gerontology Research Center and Faculty of Sport and Health Sciences, University of Jyväskylä, Finland.

Running Title: *Assessing intermuscular fat using pQCT.*

Acknowledgements: National Library of Medicine for recording the Visible Human Data Set, and granting access to the scans. The study was funded by a Deakin University Central Research Grant Scheme (CRGS) 2017 grant to AMH and SL. TR was an Academy Research Fellow during the preparation of this manuscript (Academy of Finland grant numbers 321336 and 328818). NHH is supported by a Cancer Council of Western Australia Research Fellowship. The source code of the implementation used in the present study is available from github (https://github.com/tjrantal/pQCT, commit cec9bce onwards).

Corresponding Author:

Dr. Timo Rantalainen – PhD.

Gerontology Research Center

University of Jyväskylä

Email: timo.rantalainen@jyu.fi

Abstract

INTRODUCTION: Inter/intramuscular fat can be assessed with peripheral Quantitative Computed Tomography (pQCT) and is of interest as an indicator of 'muscle quality'. Typical pQCT scan sites (forearm, lower leg) have a low amount of inter/intramuscular fat, however distal diaphyseal femur scan sites with conspicuous inter/intramuscular fat have been identified as potentially more prudent scan sites, even in healthy adolescents. However, current state of the art analysis methods require labour-intensive manual segmentation of the scan. The purpose of the present study was to evaluate the reliability of a novel open source automated enclosing convex polygon approach (source code https://github.com/tjrantal/pQCT, commit cec9bce) to quantify inter/intramuscular fat from femoral pQCT scans in healthy adults.

METHODOLOGY: The distal diaphyseal femur (25% of tibial length from the knee joint towards the hip) of twenty seven adults aged 18 to 50 years were scanned twice, one week apart, using pQCT. Subcutaneous fat, muscle, inter/intramuscular fat, and marrow areas, and corresponding densities were evaluated using a method we have reported previously, as well as the novel enclosing convex polygon method.

RESULTS: The session-to-session reliability of the assessments was fair to excellent using the previously reported method as indicated by intraclass correlation coefficient ($ICC_{2,1}$) ranging from 0.45 to 1.00, while the novel method produced excellent reliability ($ICC_{2,1}$ 0.78 to 1.00).

CONCLUSION: Distal diaphyseal femur appears to be a potentially informative and prudent scan site for inter/intramuscular fat evaluation with pQCT.

Keywords: Subcutaneous fat; soft tissue; convex hull; convex envelope; muscle; bone;

Introduction

Body fat deposits are informative e.g. of nutritional status *(1)* and may confer meaningful information in many clinical conditions *(2)*. As recently reviewed by Gruzdeva and colleagues (2018), the different fat deposits in the human body have somewhat independent metabolic roles, and may be independently associated with various clinical conditions *(2)*. Inter/intramuscular fat has been investigated as an indicator of 'muscle quality' and defined as storage of lipids in adipocytes within muscle fibres (intramuscular) or between muscle fibres and muscle groups (intermuscular) beneath the fascia of the muscle, respectively *(3)*. One of the methods utilised to evaluate intra-/intermuscular fat depots is peripheral Quantitative Computed Tomography (pQCT). The reliability of such assessments may, however, be limited *(3, 4)*. Moreover, the current state of the art analysis of intra/intermuscular fat segmentation is based on magnetic resonance or computed tomography scans through arduous manual segmentation *(3, 5)* and therefore, a more convenient, at least semi-automated, assessment method would be advantageous.

One of the reasons why pQCT-based intra/intermuscular fat assessments have undesirable reliability *(4)* may be because the typical lower leg and forearm scan sites *(6)* have, anecdotally, very low amounts of said fat even in obese older population groups. This potential pitfall could be overcome by considering alternative scan sites. Even a brief exploration of the Visible Human Data Set (Visible Human Female and Male) *(7)* cryosection images reveals that thigh cross-sections closer to the knee joint (distal) exhibit significantly greater amounts of intermuscular fat

than the other typically utilised scan sites even amongst apparently healthy adults scanned post mortem. Observably (Figure 1), one can see that muscles are encapsulated by a sheet of connective tissue (fascia), and some of the fat that appears to be connected to, or attributed to, subcutaneous fat is actually contained within the sheet encircling the muscles. In addition, conspicuous fatty infiltration along the fasciae separating muscle compartments is evident. However, in computed tomography scans, this fat may be apparently contiguous with subcutaneous fat because the connective tissue sheet is not visible (Figure 1 and Figure 2. Presumably following the reasoning above, Blew and colleagues evaluated specific fat compartments (including inter/intramuscular fat) from repeated femoral pQCT scans in adolescent girls using manual segmentation of the muscle compartment, and found acceptable concurrent validity compared to magnetic resonance imaging *(5)*. However, automated approaches to delineate subcutaneous and inter/intramuscular fat from femoral pQCT scans are currently not available.

- ENTER FIGURE 1 and FIGURE 2 -

If muscle tissue was segmented according to volumetric density, and the enclosing convex hull was subsequently defined, the delineation between inter/intramuscular fat and subcutaneous fat could be fully automated. Such an approach has not been tested and therefore the purpose of the present study was to develop and automated enclosing convex polygon based segmentation method and to evaluate the session-to-session reliability of the proposed method.

Based on the typical anatomy (Figure 1) it was hypothesised that such an approach might provide a reasonably reliable assessment of inter/intramuscular fat.

Materials and Methods

Twenty seven adults (18 males, 9 females) aged 18 to 50 years-of-age were asked to attend two scanning sessions 6 to 10 days apart, at the Deakin University, Burwood campus. The study was approved by the Deakin University Human Research Ethical Committee (2017-023), and the study was conducted in agreement with the Helsinki Declaration (World Medical Association). Written informed consent was obtained from each potential participant prior to enrolment into the study.

A pQCT scan (slice thickness 2.3 mm, in-plane voxel size 0.5 x 0.5 mm, scanning speed 30 mm/s, XCT 3000, Stratec Medizintechnik GmbH, Pforzheim, Germany) from the distal third of the thigh was obtained in each session. Following the conventions found from previous pQCT-based literature the slice obtained at the distal femoral shaft was defined as 25% of tibial length from the mid-condylar cleft towards the hip *(6)*. Tibial length was measured using a measuring tape as the distance between the most distal palpable aspect of the medial malleolus and the tibial plateau palpated from the medial side of the knee while the knee was flexed to a right angle and the lower leg was rotated externally.

Soft-tissue analysis

Two analysis approaches were applied in this study. A method we have previously reported *(8)* in addition to a novel method that was developed. In brief, in the previously reported method a 7x7 median filter is applied. All objects in the image are traced along the -40 mg/cm³ contour and subsequently flood-filled. The largest object is chosen as the limb, and everything outside this object is set to the minimum value of the image. Three layers of pixels are then eroded using a four-connected neighbourhood to account for the high-intensity pixels caused by skin. All objects with volumetric density ≥ 40 mg/cm³ are then traced along the 40 mg/cm³ contours, sorted according to the area of the object and included in muscle area provided that the area to be added is larger than 1% of the total area already included as muscle. This approach is used to exclude veins visible within the subcutaneous tissue. On occasion this approach does include large veins (e.g. varicose veins). Bone area(s) are then defined by tracing along 200 mg/cm³ contours and removed from the muscle area. Any pixels between -40 and 40 mg/cm³ within the remaining muscle area are then designated as inter/intramuscular fat. The limb area excluding muscle and bone areas is defined as subcutaneous fat, and marrow is defined as pixels within the bone area < 80 mg/cm³. Limb area, density weighted fat percentage, subcutaneous fat area, muscle area, inter/intremuscular fat area marrow area, and corresponding volumetric densities are reported as outcomes.

The novel automated enclosing convex polygon method was implemented by modifying the Density distribution *(9)* BoneJ *(10)* ImageJ *(11)* plug-in (source code available at

https://github.com/tjrantal/pQCT, commit cec9bce onwards). The implementation has multiple steps with the aim to segment soft-tissues within the scan into subcutaneous fat, inter/intramuscular fat, muscle, and marrow (marrow segmentation has not been modified from the previously reported method). The first steps are the ones outlined above up until, and including, defining muscle area by adding objects larger than 1% of the total area already included as muscle. The next step depends on using the bone centre as the origin, with the largest bone area defined as the bone to consider. The centre of the considered bone area is then used as the origin for the subsequent step. The radii from the origin of the bone area to the farthest muscle pixel (defined as the farthest distance to an image corner from the origin) was identified by starting from maximum radius away from the origin, and decrementing the radius by 0.1 pixels until a muscle pixel was found. A polar coordinate (theta: θ, radius: *R*) system was used and the procedure was repeated 720 times, i.e. every 0.5 degrees, and starting from θ = 0. Finally, the convex hull was produced using an iterative approach with the farthest radius from the previous step as the starting point. The purpose of the iterative procedure was to check whether a line can be drawn between two points on the muscle border without the line crossing muscle pixels. Line crossing search was initiated 45^{o} away from the current starting point, and the angular distance was decremented by one step (equivalent to 0.5^{o}) until a line could be drawn without going through muscle area. This point was then used as the next starting point. This algorithm was iterated until the initial starting point was encountered. As a result of the procedure, the convex hull surrounding the muscle tissues was identified. The convex hull was then filled in with a value of one into an initially empty (all values zero) mask, and the fill was subsequently dilated into any connected pixels with a volumetric density ≥ 40 mg/cm^3. A final muscle area mask was

created by setting all bone areas within the mask to zero. Any pixels with volumetric density less than 40 mg/cm³ within the muscle area mask were considered intermuscular fat, and the remaining pixels were considered muscle. Subcutaneous fat area was then defined similarly to the previously reported method. Subcutaneous fat area, muscle area, and inter/intramuscular fat area and corresponding densities are reported as outcomes from the enclosing convex polygon method.

Statistical analysis

Mean (SD) are presented as descriptive characteristics, where appropriate. Based on the analysis presented by Glüer and colleagues, an N = 27 tested on two occasions provided reasonable estimates of reliability *(12)*. Reliability was evaluated using paired t-tests, Pearson correlation coefficient (r), root mean squared coefficient of variation percentage ($CV\%_{RMS}$), and intra-class correlation coefficient (calculated for absolute agreement, $ICC_{2,1}$). ICCs were used to describe the correspondence as poor (< 0.40), fair (0.40 to < 0.60), good (0.60 to <0.75) or excellent (≥0.75) *(13)*. Statistical analysis was conducted using Matlab (version 9.1.0.441655, R2016B, MathWorks Inc., USA) and the significance level was set at $p \leq 0.05$.

Results

The mean age of the participants was 28.7 (7.1) years-of-age, and the mean tibial length was 427 (23) mm. The soft-tissue characterisation results and indicators of session-to-session reliability

are given in Tables 1 and 2. Using our previously described method, excellent reliability was observed for all explored variables (ICC = 0.78 to 1.00) but inter/intramuscular fat area (ICC = 0.7) and density (ICC = 0.45). All of the explored characteristics had excellent reliability with the novel enclosing convex polygon method (ICC = 0.79 to 1.00). Paired t-test indicated a significant 1.5% difference between measurement sessions in subcutaneous fat area when the novel method was evaluated for bias (p = 0.017).

- ENTER TABLE 1 and TABLE 2 -

Discussion

A novel fully automated soft-tissue characterisation algorithm for distal femoral pQCT scans was presented in this paper, and found to, for the most part, produce excellent reliability in estimating soft-tissue characteristics from session-to-session in healthy adults. The sole exception was muscle density, which, while categorised as excellently reliable, was conspicuously less reliable than the other assessed soft-tissue characteristics. The novel enclosing convex polygon method produced more reliable inter-/intramuscular fat estimates than the method we have previously reported.

Excellent reliability was observed for inter-/intramuscular fat evaluation with the novel method, whereas the method we have reported previously *(8)* produced good reliability for area and only

fair reliability for density. A likely culprit for the discrepancy between the methods is visible in Figure 2. The mass of intermuscular fat connected with subcutaneous fat in the sample figure could be easily encircled by muscle in a second scan, thus producing a marked difference between the estimates. It is worth noting that this limitation in the previously reported method affects femoral scans more than forearm, upper arm or lower leg scans because of the greater amount of intermuscular fat present in the distal thigh. Previous explorations of reliability of inter-/intramuscular evaluation based on pQCT scans have used tibial shaft as the scan site and reported poor reliability for area evaluation ($CV\%_{RMS}$ = 28%) with the method we have previously reported *(4)*, which is similar to the findings from the femoral scan in the present analysis. Moreover, the coefficient of variation for inter-/intramuscular fat area with the method we have previously reported was higher than what Frank-Wilson and colleagues reported for tibial scans *(4)*, which may be caused by the measurement-site specific limitation described above. Using the enclosing convex hull overcame this limitation. However, excellent reliability ($CV\%_{RMS}$ = 3.3%), indeed better than what we found with the novel enclosing convex hull method, was reported by Frank-Wilson and colleagues from tibial scans by utilising the measured pixel values as is from within the muscle area *(4)*. The discrepancy in the reliability estimates between the previous method we reported, the present method and the method reported by Frank-Wilson and colleagues *(4)* is probably explained by the difference in smoothing. That is, the excellent reliability for tibial scan inter/intramuscular fat evaluation reported by Frank-Wilson and colleagues *(4)* was based on analysis without smoothing. Despite the excellent reliability, this may be less than optimal analysis approach because a pQCT scan has visible impulse noise (e.g. Figure 1 pane C). The noise will cause many pixels within the muscle area to register as

inter/intramuscular fat, and the consistency from session-to-session in the absence of smoothing may be more an indication of consistent noise rather than actual inter/intramuscular fat. In the enclosing convex hull method presented in the present paper, the effects of the noise are minimised by applying a 7x7 median filter as recommended by Sherk and colleagues based on their exploration of filtering on the validity of pQCT soft-tissue analyses *(14)*. In effect, the remaining inter/intramuscular pixels comprise contiguous areas of fat penetrating between muscle compartments with a few intramuscular specs (e.g. Figure 2). Blew and colleagues have established the validity of pQCT assessments of thigh inter/intramuscular fat *(5)*, and with the excellent reliability, this measurement site seems to offer a feasible assessment site to evaluate subcutaneous and inter/intramuscular fat.

We observed a small (1.5%) but significant difference in subcutaneous fat area between sessions utilising the enclosing convex hull method. On closer inspection of results, this difference was driven by two participants (if these participants were removed from the analysis, no significant difference was observed between sessions [p = 0.052]) who had observable visible motion artefact (we categorised the scans into category II using the five-category scale presented by Blew and colleagues, where I is no visible artefact *(15)*) in their follow-up scan but no visible motion artefact at the baseline. The streaking caused by motion extended into the subcutaneous area and was more prominent than surrounding muscle area (i.e. farther from the centre of the bone used as the origin for the analysis). Therefore, the enclosing convex hull used the peak of the streak as a point, and consequently extended inter/intramuscular area into the subcutaneous area. This was observed as a corresponding change in inter/intramuscular area estimate as well,

but, due to the slightly poorer reliability, did not cause a significant difference between sessions. Motion artefact is a recognised issue in pQCT analysis for both hard- *(15, 16)* and soft-tissue *(17)*, and it seems that soft-tissue analyses are particularly susceptible to motion artefact (for comparison, we analysed reliability of femoral cortical cross-sectional area [ICC = 1.00, $CV\%_{RMS}$ = 1.3] from the present dataset). Based on these findings, we suggest that, if soft-tissue analyses are of interest, one should stabilise the participant as securely as feasible and be particularly vigilant for signs of motion artefact while scanning with pQCT.

Some of the limitations of the study that should be kept in mind when considering the present findings include that the participants included only apparently healthy young to middle-aged adults and therefore the results may not be generalisable to particular clinical populations with e.g. individuals with abnormally low or high adiposity. In addition, although the participants were requested to not participate in strenuous physical activity 24 h prior to the testing sessions (as per our standard laboratory protocol), no effort was made to enforce that resistance training was not engaged in prior to one or the other of the testing sessions. Similarly, there was no standard duration of a particular posture required for a period of time prior to scanning. Therefore potential effects of muscle and adipose tissue swelling caused by exercise induced muscle damage or gravity-caused fluid shifts cannot be ruled out. Finally, the size of the pQCT device gantry varies by model, and in adults it may be difficult to scan the distal femoral scan site with models other than the XCT 3000.

In conclusion, distal thigh pQCT scans were found to afford reliable estimation of muscle, subcutaneous fat, inter/intramuscular fat and medullary fat in healthy adults using the automated enclosing convex hull segmentation approach. Validity and reliability now needs to be established in specific populations, and special care needs to be taken to minimise motion artefact if utilising the presented method.

REFERENCES

1. Fischer M, JeVenn A, Hipskind P. 2015 Evaluation of Muscle and Fat Loss as Diagnostic Criteria for Malnutrition. Nutr Clin Pract. 30:239–248.

2. Gruzdeva O, Borodkina D, Uchasova E, Dyleva Y, Barbarash O. 2018 Localization of fat depots and cardiovascular risk. Lipids Health Dis. 17:218.

3. Erlandson MC, Lorbergs AL, Mathur S, Cheung AM. 2016 Muscle analysis using pQCT, DXA and MRI. Eur J Radiol. 85:1505–1511.

4. Frank-Wilson AW, Johnston JD, Olszynski WP, Kontulainen SA. 2015 Measurement of muscle and fat in postmenopausal women: precision of previously reported pQCT imaging methods. Bone. 75:49–54.

5. Blew RM, Lee VR, Bea JW, et al. 2018 Validation of Peripheral Quantitative Computed Tomography–Derived Thigh Adipose Tissue Subcompartments in Young Girls Using a 3 T MRI Scanner. J Clin Densitom. 21:583–594.

6. Cervinka T, Giangregorio L, Sievanen H, Cheung AM, Craven BC. 2018 Peripheral Quantitative Computed Tomography: Review of Evidence and Recommendations for Image Acquisition, Analysis, and Reporting, Among Individuals With Neurological Impairment. J Clin Densitom. 21:563–582.

7. Ratiu P, Hillen B, Glaser J, Jenkins DP. 2003 Visible Human 2.0--the next generation. Stud Health Technol Inform. 94:275–281.

8. Rantalainen T, Nikander R, Heinonen A, Cervinka T, Sievänen H, Daly RM. 2013 Differential Effects of Exercise on Tibial Shaft Marrow Density in Young Female Athletes. J Clin Endocrinol Metab. 98:2037–2044.

9. Rantalainen T, Nikander R, Heinonen A, Daly RM, Sievanen H. 2011 An open source approach for regional cortical bone mineral density analysis. J Musculoskelet Neuronal Interact. 11:243–248.

10. Doube M, Kłosowski MM, Arganda-Carreras I, et al. 2010 BoneJ: Free and extensible bone image analysis in ImageJ. Bone. 47:1076–1079.

11. Schneider CA, Rasband WS, Eliceiri KW. 2012 NIH Image to ImageJ: 25 years of image analysis. Nat Methods. 9:671–675.

12. Glüer C-C, Blake G, Lu Y, Blunt BA, Jergas M, Genant HK. 1995 Accurate assessment of precision errors: How to measure the reproducibility of bone densitometry techniques. Osteoporos Int. 5:262–270.

13. Cicchetti DV. 1994 Guidelines, criteria, and rules of thumb for evaluating normed and standardized assessment instruments in psychology. Psychol Assess. 6:284.

14. Sherk VD, Bemben MG, Palmer IJ, Bemben DA. 2011 Effects of filtering methods on muscle and fat cross-sectional area measurement by pQCT: a technical note. Physiol Meas. 32:N65-72.

15. Blew RM, Lee VR, Farr JN, Schiferl DJ, Going SB. 2014 Standardizing Evaluation of pQCT Image Quality in the Presence of Subject Movement: Qualitative Versus Quantitative Assessment. Calcif Tissue Int. 94:202–211.

16. Rantalainen T, Chivers P, Beck BR, et al. 2018 Please Don't Move-Evaluating Motion Artifact From Peripheral Quantitative Computed Tomography Scans Using Textural Features. J Clin Densitom Off J Int Soc Clin Densitom. 21:260–268.

17. Wong AKO. 2016 A comparison of peripheral imaging technologies for bone and muscle quantification: a technical review of image acquisition. J Musculoskelet Neuronal Interact. 16:265–282.

FIGURE LEGENDS

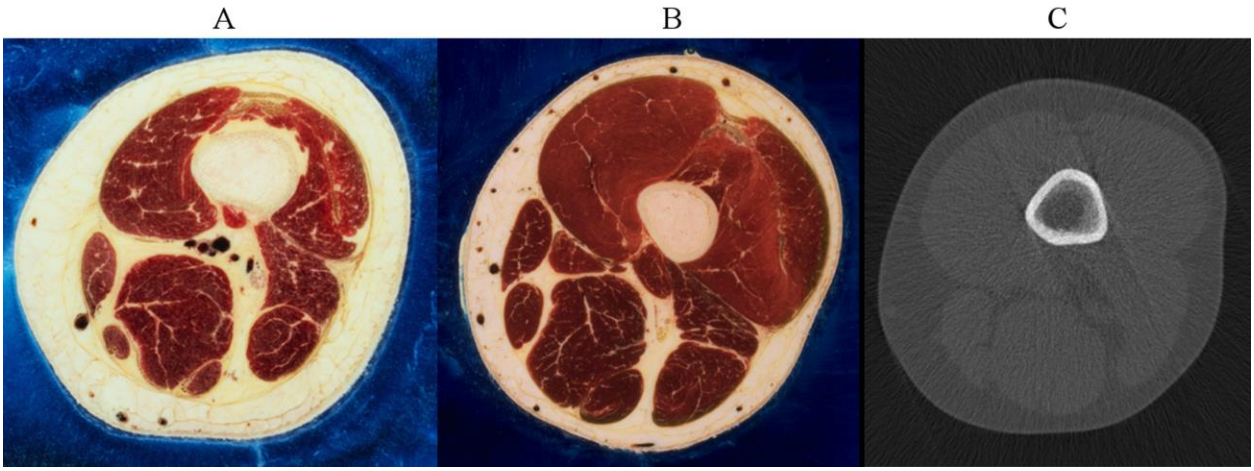

Figure 1. Pane A; image number 4435 of the visible female project 70mm cryosection images, which is approximately three quarters along the length from the femoral neck to the knee joint. Pane B; image number 2203 of the visible man project 70mm cryosection images, which is approximately three quarters along the length from the femoral neck to the knee joint. Note the conspicuous colour difference between intermuscular and subcutaneous fat, and the connective tissue sheet separating the compartments from each other. Pane C; a sample peripheral quantitative computed tomography scan from a similar scan site. Note how the connective tissues are indistinguishable from fat and that no apparent difference can be seen between intermuscular and subcutaneous fat tissues.

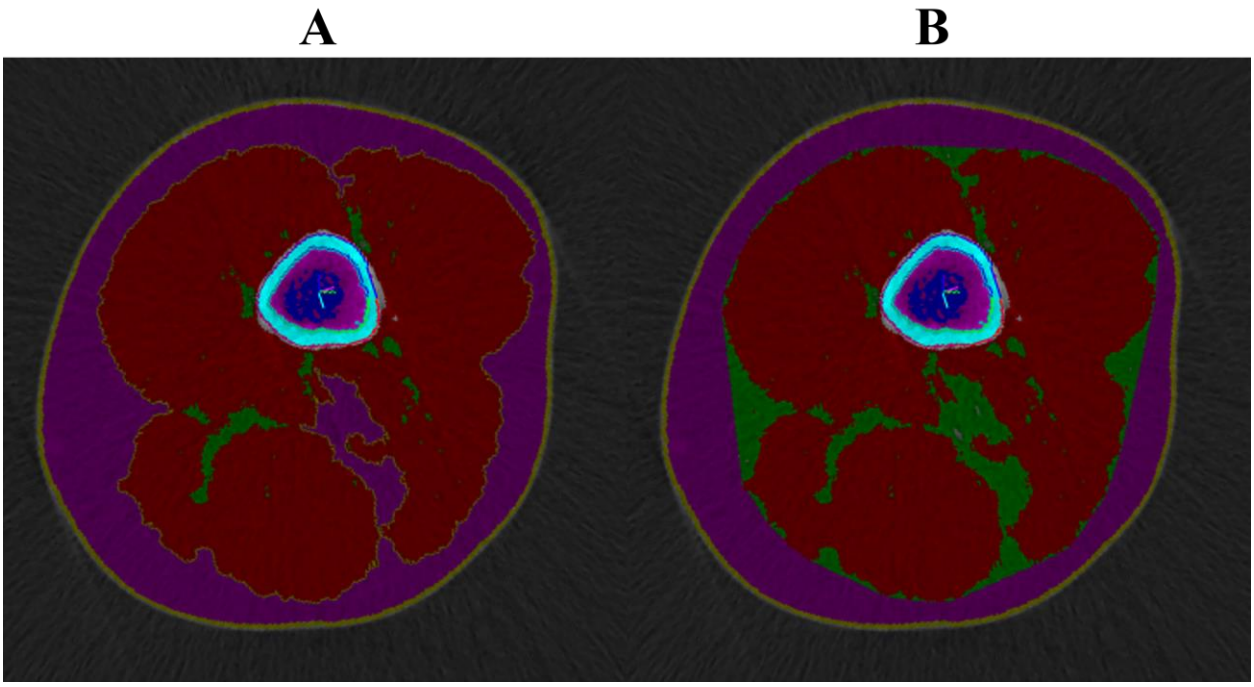

Figure 2. Pane A; pQCT scan analysed with simple thresholds of fat and muscle. Note the intermuscular area connected to subcutaneous tissue and tinted purple below the femur. Pane B; the same scan analysed with the proposed enclosing convex polygon algorithm. Note that the intermuscular area, which was connected to the subcutaneous area in the left pane, is tinted with green, which indicates inter/intramuscular fat. Note also the areas on the lateral and medial aspects of the scan indicated as inter/intramuscular fat due to the enclosing convex polygon segmentation approach.

TABLES

Table 1. Thigh soft-tissue characteristics and reliability indicators based on the previously reported analytical approach.

	Mean					
	Session 1	Session 2	Bias (95% LoA)	Bias p-value	ICC (95% CI)	$CV\%_{rms}$
Muscle Density [mg/cm³]	77.6 (1.8)	77.9 (1.9)	0.3 (-2.1 to 2.7)	0.228	0.78 (0.57 to 0.89)	1.1
Muscle Area [cm²]	83.4 (21.7)	83.1 (22.2)	-0.3 (-4.5 to 4.0)	0.535	1.00 (0.99 to 1.00)	1.9
Intramuscular Fat Density [mg/cm³]	20.9 (4.9)	20.4 (5.6)	-0.5 (-11.3 to 10.3)	0.637	0.45 (0.09 to 0.71)	21.0
Intramuscular Fat Area [cm²]	3.38 (2.14)	3.46 (2.25)	0.09 (-3.31 to 3.48)	0.792	0.70 (0.43 to 0.85)	38.0
Subcutaneous Fat Density [mg/cm³]	2.46 (6.85)	2.42 (7.20)	-0.04 (-2.73 to 2.64)	0.870	0.98 (0.96 to 0.99)	92.6
Subcutaneous Fat Area [cm²]	30.9 (14.6)	30.7 (14.6)	-0.2 (-3.7 to 3.3)	0.534	0.99 (0.98 to 1.00)	5.8
Medullary Density [mg/cm³]	22.0 (5.3)	21.5 (5.7)	-0.5 (-7.4 to 6.4)	0.460	0.80 (0.61 to 0.90)	11.8
Medullary Area [cm²]	1.12 (0.86)	1.13 (0.85)	0.01 (-0.20 to 0.21)	0.757	0.99 (0.98 to 1.00)	14.3
Limb Density [mg/cm³]	84.2 (13.1)	84.5 (13.3)	0.3 (-2.0 to 2.7)	0.172	1.00 (0.99 to 1.00)	1.0
Limb Area [cm²]	134 (29)	134 (30)	0 (-5 to 4)	0.416	1.00 (0.99 to 1.00)	1.2

Density weighted fat percentage [%]	28.7 (9.3)	28.6 (9.3)	0.0 (-1.5 to 1.4)	0.836	1.00 (0.99 to 1.00)	1.8

LoA = Limits of agreement; ICC = intraclass correlation coefficient calculated for absolute agreement, CI = confidence interval; CV_{rms} = Root-mean-squared % coefficient of variation

Table 2. Thigh soft-tissue characteristics and reliability indicators based on the novel enclosing convex hull analysis. Only results that are affected by the convex hull algorithm are presented.

	Mean					
	Session 1	Session 2	Bias (95% LoA)	Bias p-value	ICC (95% CI)	$CV\%_{rms}$
Intramuscular Fat Density [mg/cm^3]	17.7 (3.8)	17.6 (3.9)	-0.2 (-3.3 to 2.9)	0.577	0.92 (0.83 to 0.96)	6.5
Intramuscular Fat Area [cm^2]	9.79 (4.41)	10.07 (4.47)	0.27 (-2.24 to 2.79)	0.276	0.96 (0.91 to 0.98)	9.1
Subcutaneous Fat Density [mg/cm^3]	1.71 (6.85)	1.79 (7.80)	0.08 (-3.57 to 3.72)	0.832	0.97 (0.93 to 0.99)	108.8
Subcutaneous Fat Area [cm^2]	26.6 (13.5)	26.2 (13.7)	-0.4 (-1.9 to 1.2)	0.017	1.00 (0.99 to 1.00)	7.8

LoA = Limits of agreement; ICC = intraclass correlation coefficient calculated for absolute agreement, CI = confidence interval; CV_{rms} = Root-mean-squared % coefficient of variation